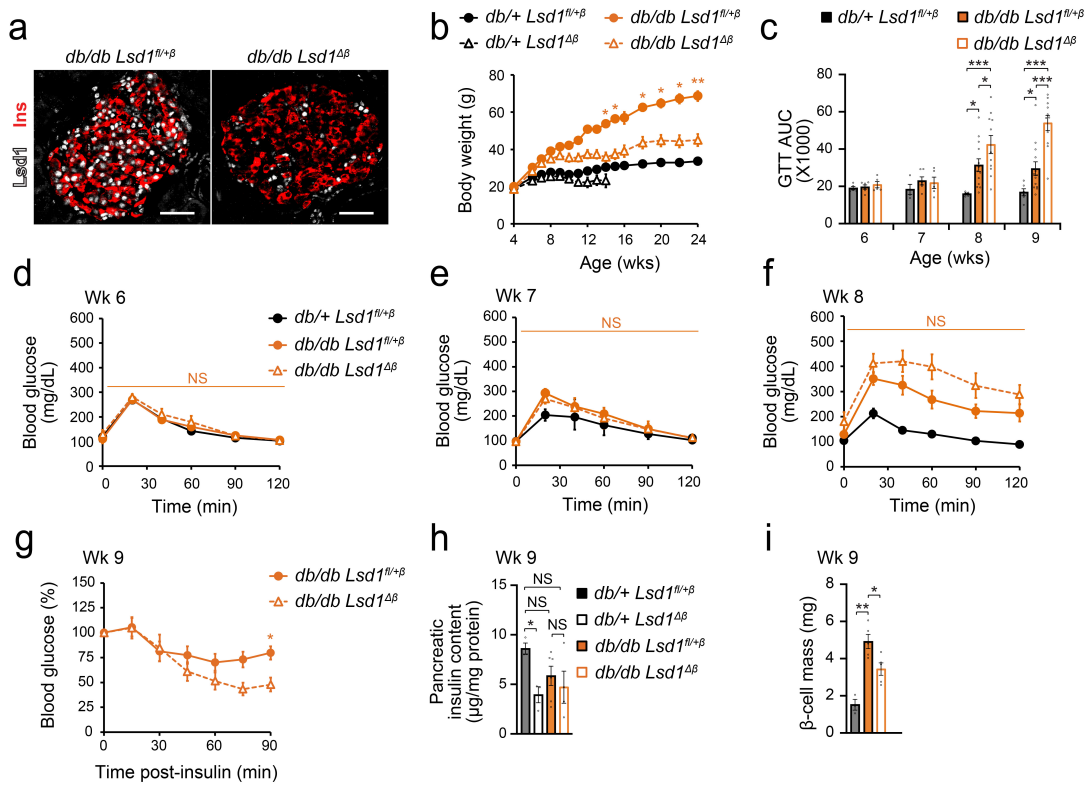


## Extended Data Figures



### Extended Data Figure 1. *Lsd1* inactivation in β-cells accelerates the onset of glucose intolerance in *db/db* mice. Related to Figure 1.

**(a)** Immunofluorescence staining for insulin (Ins) and *Lsd1* on pancreas sections from TM-treated *Lsd1<sup>fl/+β</sup>; db/db; Pdx1-CreER* (*db/db Lsd1<sup>fl/+β</sup>*) mice and TM-treated *Lsd1<sup>fl/Δβ</sup>; db/db; Pdx1-CreER* (*db/db Lsd1<sup>Δβ</sup>*) mice two days after TM treatment as in Fig. 1a. Scale bar, 50 μm. TM, tamoxifen. Representative image from *n* = 1 mouse per group.

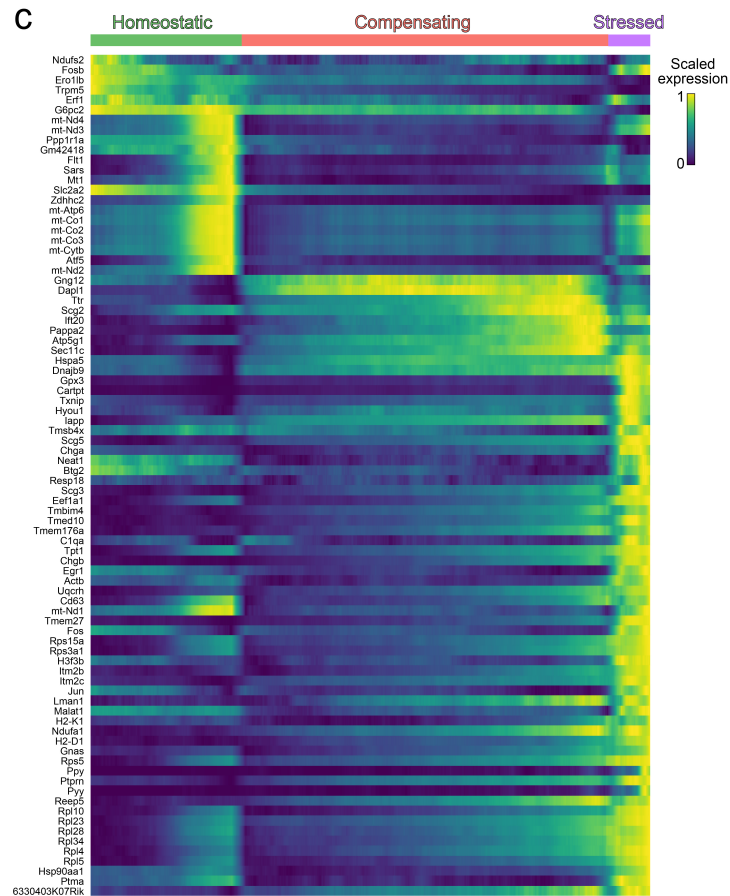
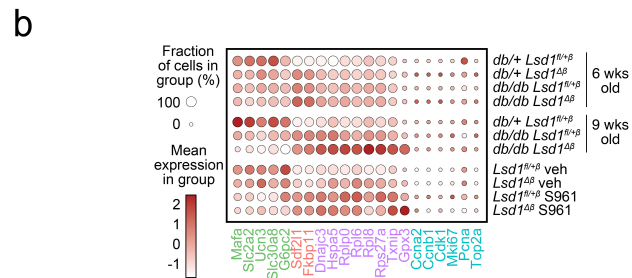
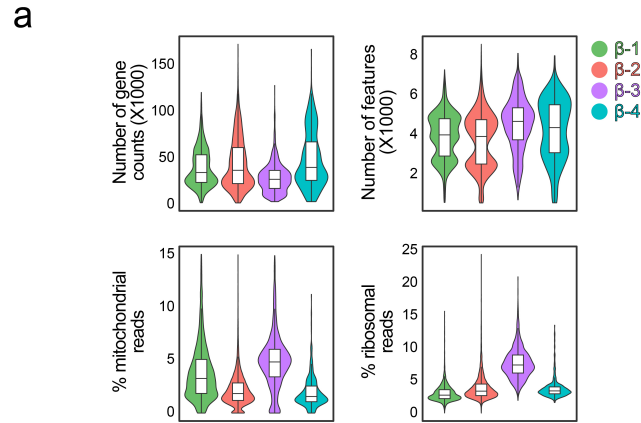
**(b)** Longitudinal body weight measurements of *db/+ Lsd1<sup>fl/+β</sup>* (*n* = 7), *db/+ Lsd1<sup>Δβ</sup>* (*n* = 14), *db/db Lsd1<sup>fl/+β</sup>* (*n* = 8), and *db/db Lsd1<sup>Δβ</sup>* (*n* = 11). Wks, weeks. \**p*<0.05, \*\**p*<0.01 between *db/db Lsd1<sup>fl/+β</sup>* and *db/db Lsd1<sup>Δβ</sup>* mice.

**(c - f)** Longitudinal glucose tolerance tests in mice of the indicated genotypes shown as (c) area under the curve (AUC) for all time points or (d - f) blood glucose levels following intraperitoneal glucose injection for each time point. AUC, area under the curve. *db/+ Lsd1<sup>fl/+β</sup>* wk 7: *n* = 4 mice, *db/db Lsd1<sup>fl/+β</sup>* wks 6 and 7: *n* = 6 mice, *db/db Lsd1<sup>Δβ</sup>* wk 8: *n* = 11 mice, *db/db Lsd1<sup>fl/+β</sup>* wks 8 and 9: *n* = 13 mice, *db/+ Lsd1<sup>fl/+β</sup>* wk 9: *n* = 6 mice, all other groups: *n* = 5 mice. NS, not significant between *db/db Lsd1<sup>fl/+β</sup>* and *db/db Lsd1<sup>Δβ</sup>* mice.

**(g)** Insulin tolerance tests in 9-week-old *db/db Lsd1<sup>fl/+β</sup>* (*n* = 13), and *db/db Lsd1<sup>Δβ</sup>* (*n* = 11) mice. Blood glucose levels are shown relative to the 0 min time point. \**p*<0.05 between *db/db Lsd1<sup>fl/+β</sup>* and *db/db Lsd1<sup>Δβ</sup>* mice.

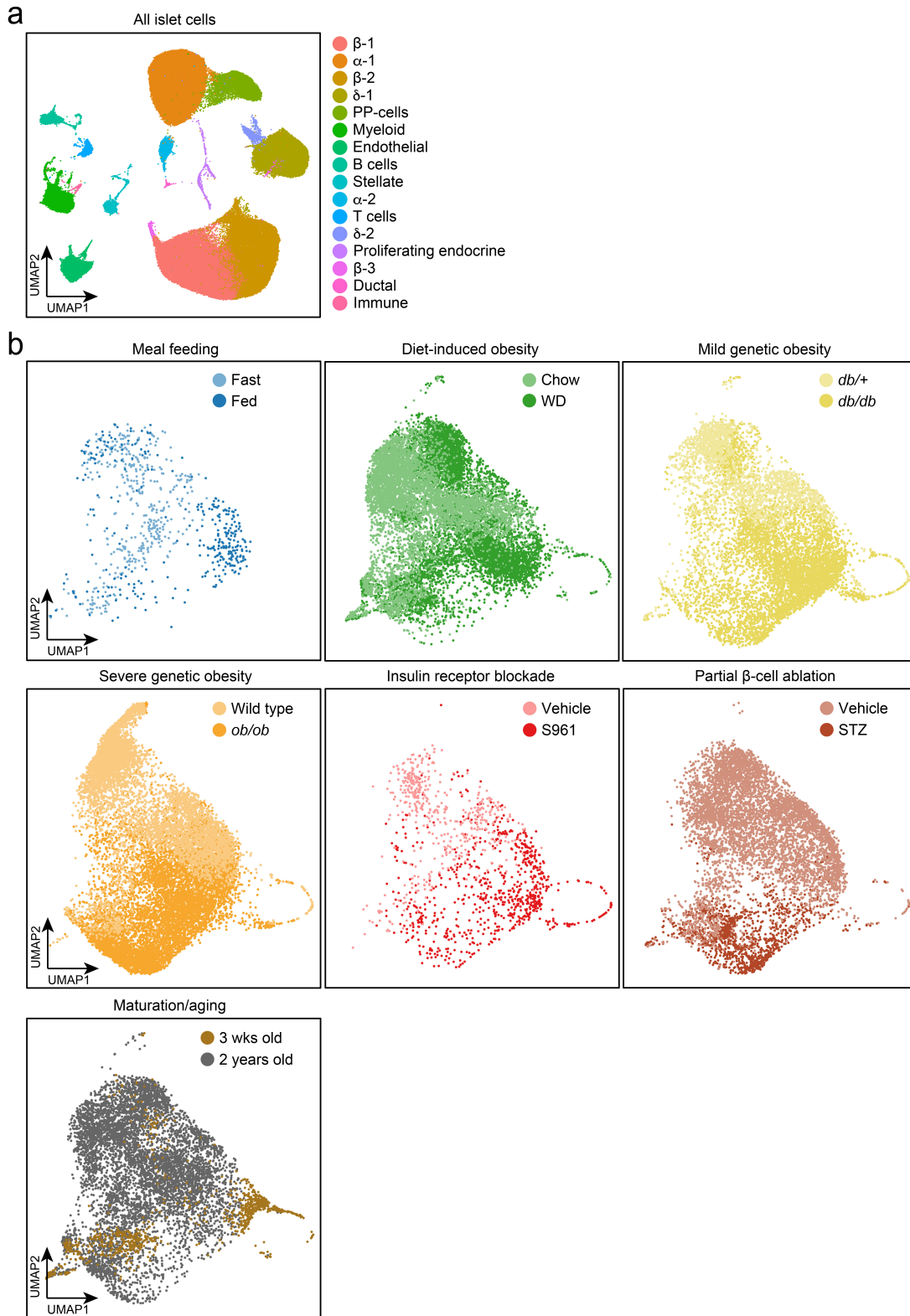
**(h and i)** Pancreatic insulin content (h) and β-cell mass (i) in 9-week-old mice of the indicated genotypes. *db/db Lsd1<sup>fl/+β</sup>*: *n* = 6 (h) or *n* = 5 (i) mice, *db/db Lsd1<sup>Δβ</sup>* *n* = 4 (h) or *n* = 5 (i) mice, all other groups: *n* = 3 mice.

Significance was determined by one-way ANOVA followed by Student's t-test with Welch's correction for unequal variance as necessary followed by Dunnett's multiple comparisons test (c, h, i) or two-way ANOVA for genotype interaction with time followed by Sidak's multiple comparisons test (b, d - g).



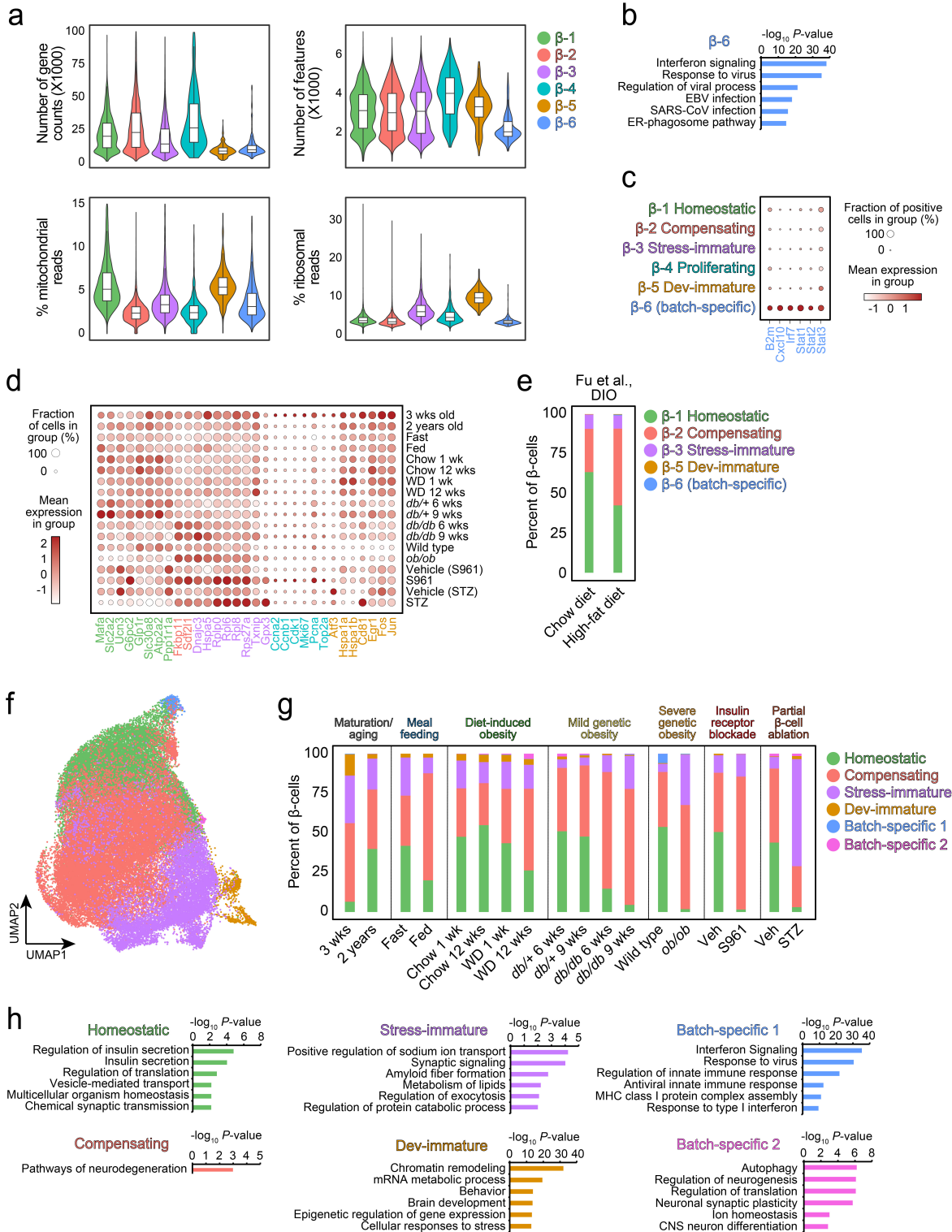
Extended Data Figure 2. Validation of  $\beta$ -cell state classifications. Related to Figure 2.

- (a) Violin plots of quality control metrics for each  $\beta$ -cell state from Fig. 2b.
- (b) Dot plot showing expression of mRNAs from Fig. 2d for each sample. Gene symbol colors indicate the state enriched for each corresponding mRNA.
- (c) mRNA expression changes along the diffusion pseudotime trajectory for the three most abundant  $\beta$ -cell states in Fig. 2b. Cells were ordered as in <sup>27</sup>.



**Extended Data Figure 3. Validation of data integration. Related to Figure 3.**

- (a)** UMAP of integrated and clustered islet cells colored by cell type and state. UMAP, uniform manifold approximation and projection.
- (b)** UMAPs of re-integrated  $\beta$ -cells from the indicated datasets colored by genotype or treatment group.

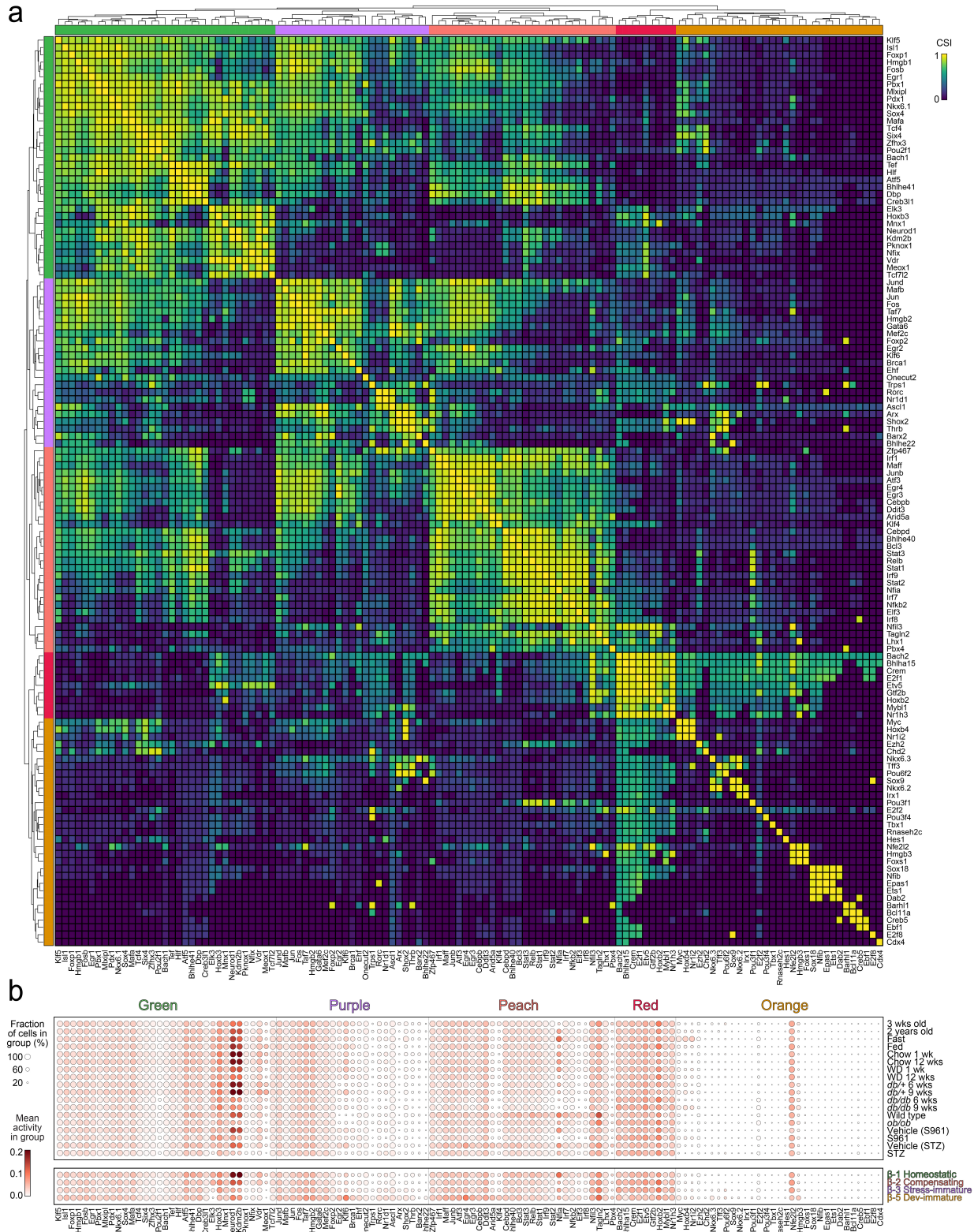


**Extended Data Figure 4. Validation of  $\beta$ -cell state classifications in the mouse islet atlas. Related to Figure 3.**

**(a)** Violin plots of quality control metrics for each  $\beta$ -cell state from Fig. 3b.

- (b)** Enriched gene ontologies and pathways for mRNAs more highly expressed in the  $\beta$ -6 subset relative to all other  $\beta$ -cells.
- (c)** Dot plot showing expression of representative mRNAs from gene ontologies and pathways selected from (b).
- (d)** Dot plot showing expression of mRNAs from Fig. 3d for each sample. Gene symbol colors indicate the state enriched for each corresponding mRNA.
- (e)** Abundance of each  $\beta$ -cell subset as a proportion of total  $\beta$ -cells for  $\beta$ -cells from chow- or high-fat diet-fed mice<sup>63</sup> mapped to the integrated dataset in Fig. 3f. DIO, diet-induced obesity.
- (f and g)** UMAP of clustered nonproliferating  $\beta$ -cells colored by state after regressing mitochondrially encoded mRNAs and ribosomal protein genes (f) and abundance of each  $\beta$ -cell state as a proportion of total  $\beta$ -cells for the indicated treatments and genotypes (g). UMAP, uniform manifold approximation and projection.
- (h)** Enriched gene ontologies and pathways for mRNAs more highly expressed in each state relative to all other  $\beta$ -cells. The top six most significantly enriched categories are shown.





**Extended Data Figure 6. Transcription factor activities correspond to distinct  $\beta$ -cell states. Related to Figure 4.**

**(a)** Correlation plot of pairwise regulon activities among nonproliferating  $\beta$ -cells from experimental groups in Fig. 3a clustered into co-expression modules using CSI (connection specificity index).

**(b)** Dot plot showing activities for the indicated regulons from (a) in nonproliferating  $\beta$ -cells from the indicated experimental groups and states.